DC Motor Behavior Analysis on Blocking the Wheels on a Railway Traction Vehicle

IOAN BACIU DRAGOŞ PĂSCULESCU CORINA DANIELA CUNȚAN ANCA IORDAN
Electrical Engineering and Industrial Informatics Department
Polytechnic University of Timisoara
Revolution str. no 5, Hunedoara, code 331170
ROMANIA
ioan.baciu@fih.upt.ro, pdragos_74@yahoo.com, corina.cuntan@fih.upt.ro, iordan.anca@fih.upt.ro,
http:// www.fih.upt.ro

Abstract: - In this work are determined the current's and voltage's values absorbed by the d.c. motor from the componency of a 5MVA locomotive in short-circuit regime. The measures are determined by means of an analyzer of electric power's quality on a locomotive from the periodic testing station. Are determined also the values of the harmonic distorsion factor and of the current's and voltage's harmonics. The acquired data recorded in the analyzer's memory are passed afterwards into a computing system that allows their further analysis.

Key-Words: electric power's quality, harmonic distorsion factor, voltage harmonics, current harmonics, d.c. motor, short-circuit regime.

1 Introduction

In three-phased systems, if one of the grid's elements or a consumer is unbalanced, the regime becomes non-symmetric.

The most unfavorable consequence of the voltage unbalance is the circulation of some additional current component (negative and zero) that lead to additional losses, parasite couples at AC electric motors, wear increase, etc.

The most important unbalances are produced by the high-power industrial single-phased consumers, connected to the medium or high voltage electric grids, e.g: transformation stations for supplying the railway electric traction, welding installations, single-phased electric furnaces, etc.[1][11][20]

The unbalanced and non-linear consumer is not using the entire power received from the generator, but only a part, the rest converting it into non-symmetry on fundamental and into deforming power, sending it to the grid and to the balanced and linear consumer, reason for which we should eliminate the unbalances and non-linearity, to reduce to minimum the circulation of non-symmetry and deforming powers.[2]

2 Theoretical Issue

The motors used at electric traction locomotives are of direct-current with serial excitation.

With the excitation circuit in series with the armature (at brushes), the d.c. brush series motor is convenient for wide constant power speed range, so needed in traction applications or ICE starters, Fig.1.

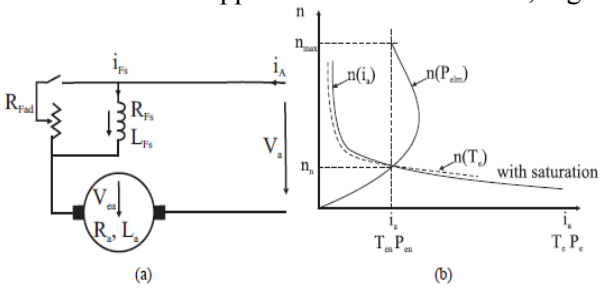

Figure 1. The d.c. brush series machine: equivalent circuit, (a), natural characteristic curves for rated voltage and no R_{Fad}(b)

This machine is used mainly as a motor and it may be used for self-excitation regenerative braking only after first switching the terminals of field winding (to reverse the excitation field).

Alternatively, the excitation may be separated first and then supplied separated (at low voltage) for regenerative braking, as done routinely on standard Diesel - electric or electric locomotives.[3]
(Recent and new traction drives use induction machines with full power electronics control).

We will deal here only with the motor mode for which the voltage equation is:

$$V_a = \left(R_a + R_{Fs}^e\right) i_a + \left(L_a + L_{Fs}\right) \frac{di_a}{dt} + V_{ea} \qquad (1)$$

Now the pole flux produced by the field current i_{Fs}, which is proportional (2) to the armature current (and equal to it when no flux weakening is

performed by adding R_{Fad} in parallel with the field winding R_{Fs}).

$$V_{ea} = K_e \cdot \Phi_p(i_{Fs})n$$

$$R_{Fs}^e = \frac{R_{Fs}R_{Fad}}{R_{Fs}+R_{Fad}} \quad (2)$$

$$i_{Fs} = i_a \frac{R_{Fad}}{R_{Fad}+R_{Fs}}$$

For steady state $di_a / dt = 0$.

The torque *Te* is:

$$T_e = \frac{V_{ea}i_a}{2\pi n} = \frac{K_e\Phi_p(i_{Fs})i_a}{2\pi} \quad (3)$$

The d.c. brush series motor may be described by the curves: $n(i_a); n(P_{em}); n(T_e); \eta(P_{em})$;

$$\eta = \frac{P_{em} - p_{mec} - p_{iron}}{P_{em} + p_{copper} + p_{brush}} \quad (4)$$

Magnetic saturation occurs above a certain i_a value and, from then on, the pole flux φ_p stays constant ant thus the characteristics at high current degenerate into those of d.c. brush separate excitation motors. Let us neglect saturation and consider a linear relationship between i_{Fs} and φ_p:

$$\Phi_p \approx K_\Phi \cdot i_{Fs} \quad (5)$$

From (1) - (4) we derive:

$$i_a = \frac{V_a}{R_a + \frac{R_{Fs}R_{Fad}}{R_{Fs}+R_{Fad}} + K_e \cdot K_\Phi \frac{R_{Fad}}{R_{Fad}+R_{Fs}} n} \quad (6)$$

$$T_e = K_e K_\Phi \frac{R_{Fad}}{R_{Fad}+R_{Fs}} i_a^2 ; P_{elm} = T_e 2\pi n \quad (7)$$

Graphical representation of the $n(ia)$, $n(T_e)$, $n(P_{em})$ is shown in Fig.1b. It is evident from eqns.(6) - (7) that the electromagnetic (developed) power shows a maximum at certain speed, for constant voltage V_a (Fig.1b). Also, the ideal no load speed is $n_{0i} \rightarrow \infty$, because at zero current the flux tends to zero (in fact to a permanent small value) φ_{prem}. So a d.c. brush series motor should not be left without load, a condition always fulfilled in traction drives. The $n(i_a)$, $n(T_e)$ are mild allowing for wide speed variation with appropriate control, to provide rigorously constant electromagnetic power over an $n_{max}/n_n = 3 : 1$ speed range.[3]

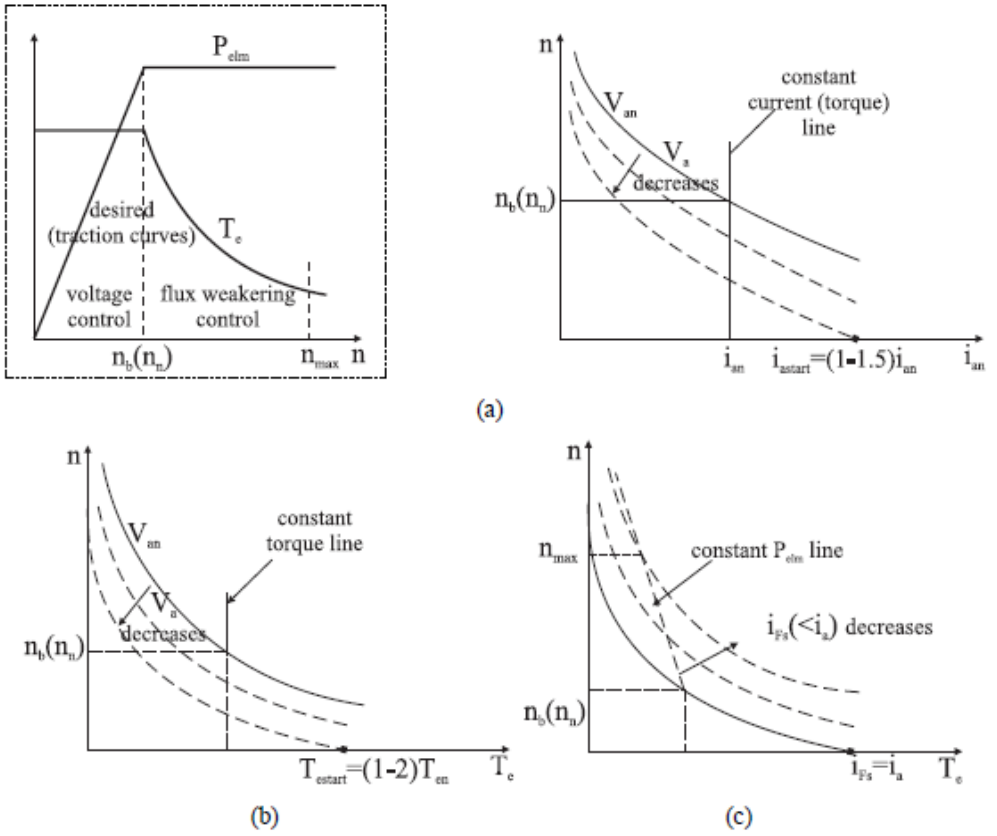

Figure 2. Speed control of d.c. brush series motor curves: traction motor torque (power) speed envelops, (a), voltage reduction control under base speed n_b for constant torque limit ($n(i_a)$ and $n(T_e)$ curves), (b), flux weakening above base speed n_b for constant P_{elm} limit,(c).

Two effective methods of starting (limiting the current) and speed control are visible (for given torque) from (6) - (7):

* Voltage control (by voltage reduction below V_{an}): $n < n_n$

The torque at given speed is proportional to voltage squared (with neglected saturation) and thus the $n(i_a)$, $n(T_e)$ curves fall below those at V_{an} if $V_a < V_{an}$, to produce the desired Brush - commutator machines: steady-state 4-39 current (torque) at any speed below rated speed *nn* (Fig.2a). For example, constant torque up to base (rated) speed may be provided this way (Fig.2b).

Field weakening speed control ($n_n < n < n_{max}$). By modifying step-wise the resistance R_{Fad} in parallel with the field winding R_{Fs}, the field current i_{Fs} becomes smaller than armature current i_a and thus flux weakening occurs. Above base speed we may modify R_{Fad} (Fig.1a) such that to maintain $P_{elm} = P_{en}$, if so desired, up to maximum speed n_{max} (Fig.2c). [3]

The universal motor is a.c. series excited at constant (grid) frequency, but at variable voltage amplitude, for speed control. For home appliances or construction tools (below 1kW), a triac a.c. voltage changer (soft starter) produces the required voltage. For 2(3) fixed speeds simpler appliances, winding tapping or additional series resistance is used.

Right after 1900, universal motors in the tenths of kW, with variable output voltage tapping of winding under load), in configurations provided with interpoles and series compensation or short circuit (fig.3), have been used in Switzerland, for example, on mountain railroads locomotives at 16.33Hz; some of them are apparently still in use today.[3]

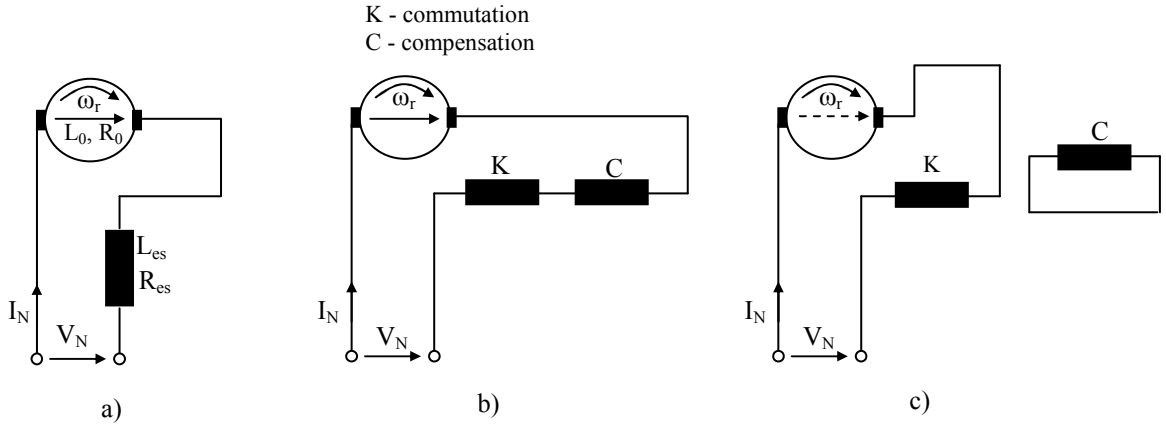

Figure 3. A.C. brush series motor: low power, (a), medium power with series compensation *C*, (b), medium power with shortcircuit compensation *C*;*K* - inter-pole (commutation) winding, (c).

The machine voltage equation is taking notice that the a.c. excitation induces a pulsation V_{ep} and motion emf Ver into the rotor circuit:

$$(R_a + R_{Fs})i - V = V_{ep} - V_{er} \quad (8)$$

The pulsation (transformer - like) self induced voltage (emf) Vep is:

$$V_{ep} = -(L_a + L_{Fs})\frac{di}{dt} \quad (9)$$

The motion emf V_{er} is, as in d.c., with neglected magnetic saturation:

$$V_{er} = K_e n \phi_p \cong K_e K_\phi n i \quad (10)$$

The electromagnetic torque T_e, as for d.c., is:

$$T_e(t) = \frac{V_{er} i}{2\pi n} \cong \frac{K_e K_\Phi i^2}{2\pi} \quad (11)$$

The torque expression resembles the formula for the d.c. brush series motor, but the current is a.c. and, during steady state, at stator (supply) frequency ω1.For steady state (constant speed, constant torque load):

$$V(t) = V_1\sqrt{2}\cos\omega_1 t$$
$$i(t) = I_1\sqrt{2}\cos(\omega_1 t - \varphi_1) \quad (12)$$

Current i in the stator and at rotor brushes is indeed at frequency ω_1, but, in the rotor, one more frequency $\omega_\gamma = 2\pi n p_1 =$ occurs as in a.c. brush machines.

For rated speed $\omega_\gamma = (3-6)\omega_1$, in order to secure large motion emf, V_{er}, which, being in phase with the current, leads to a very good power factor. Now with (12) in (11) the instantaneous steady state torque $T_e(t)$:

$$T_e(t)=\frac{K_e K_\Phi I_1^2}{2\pi}\left(1-\cos 2(\omega_1 t-\varphi_1)\right) \quad (13)$$

As expected, from a single phase winding a.c. machine (of any kind), the torque pulsates at 2ω1 and care must be exercised in damping the frame vibration due to it. As with a.c. sinusoidal terminal voltage and current circuits (leaving out the true $\omega_1+\omega_\gamma$ frequency in the rotor), phasors may be used:

$$v\rightarrow \underline{V}=V_1\sqrt{2}\cdot e^{j\omega_1 t};\quad i\rightarrow \underline{I}=I_1\sqrt{2}e^{j(\omega_1 t-\varphi_1)} \quad (14)$$

With (14) in (8) - (10) we obtain:

$$\underline{V}=(R_a+R_{FS})\underline{I}+j\omega_1(L_a+L_{FS})\underline{I}+K_e K_\phi N\underline{I} \quad (15)$$

With $R_a+F_{Fs}=R_{ae};\ \omega_1(L_a+L_F)=X_{ae}$ and introducing a series resistance R_{iron} to account for iron losses (both in the stator and rotor),(15) becomes:

$$\underline{V}=\underline{I}\left(R_{ae}+jX_{ae}+R_{iron}+K_e K_\phi n\right) \quad (16)$$

The average torque T_{eav} (from 13) is simply:

$$T_{eav}=\frac{K_e K_\phi I^2}{2\pi};\quad \cos\varphi=\frac{\left(R_{ae}+R_{iron}+K_e K_\phi n\right)I}{V} \quad (17)$$

with current from (16) in (17) the torque speed curve is:

$$T_e an=\frac{K_e K_\Phi}{2\pi}\frac{V^2}{(R_{ae}+R_{iron}+K_e K_\Phi n)^2+X_{ae}^2} \quad (18)$$

The n (T_{ean}) curve (fig.4.) resembles the d.c. brush series motor and speed control is handled by amplitude voltage control easily through a triac softstarter (with an adequate power filter to attenuate harmonics current in the rather weak (residential) power sources (transformers)).

As already explained in the paragraph on commutation, a.c. current commutation is more difficult because of the additional a.c. excitation emf in the commuting coil, present at all speeds. This a.c. emf has to be reduced below 3.5V at start and to 1.5 − 2.5V at full speed running.

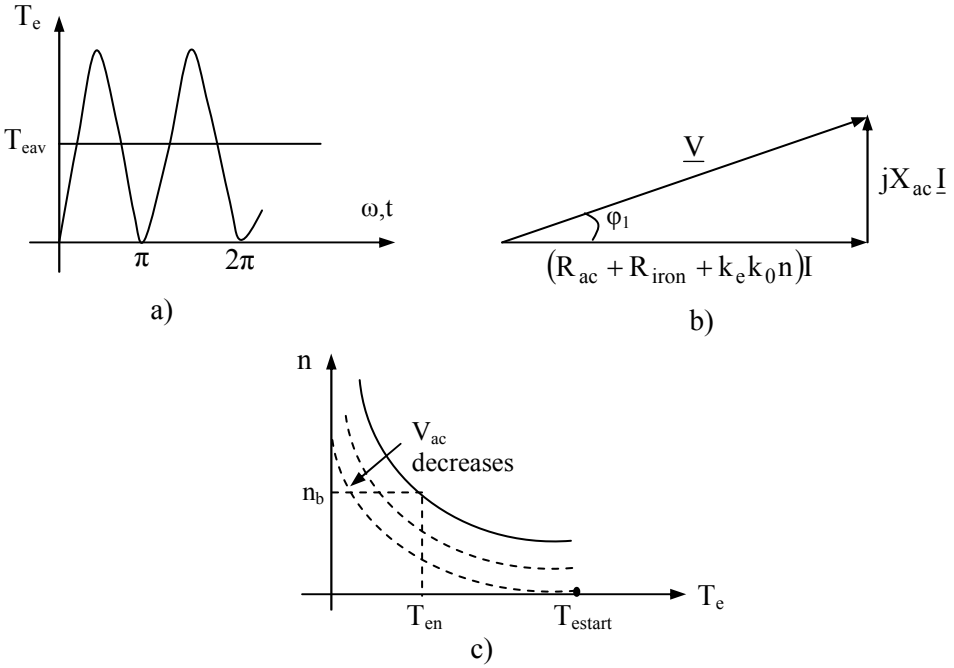

Figure 4. The a.c. brush series (universal) motor characteristics: Instantaneous torque pulsations at $2\omega_1$ frequency, (a), The phasor diagram at rated speed: $\cos\varphi_1 > 0.9$ for $(p1nn/f1)\approx(3\div 6)$, (b), Speed control by ac. voltage reduction: n(T_{ean}) curves, (c).

Frequency reduction is another way to improve commutation, the main design limiting factor. Due to overall reduced cost, the universal motor is still heavily used in home appliances from hair dryers to vacuum cleaners and some washing machines and for hand-held tools with dual or variable speed. One contemporany automotive small d.c. brush PM motor and one hand-held tool universal motor are shown in fig.4.

Determinations of the current harmonics, as well as the THD factor, are made with a three-phased energy analyzer which allows the computing of these parameters according to the following relations.

RMS values for voltage and current:

$$V_{rms}(i)=\sqrt{\frac{1}{N}\cdot\sum_{n=0}^{N}V(i,n)^2} \quad (19)$$

where: N represent the number of samples for the acquisition time;

V_{rms} single RMS voltage $i+1$ phase;

$\mathrm{Vavg[i]=Vrms[i]}$

$$U_{rms}(i)=\sqrt{\frac{1}{N}\cdot\sum_{n=0}^{N}U(i,n)^2} \quad (20)$$

where: U_{rms} compound RMS voltage $i+1$ phase $U_{avg}(i)=U_{rms}(i)$

$$A_{rms}(i)=\sqrt{\frac{1}{N}\cdot\sum_{n=0}^{N}A(i,n)^2} \quad (21)$$

where: $\mathrm{Arms(i)}$ - Effective current phase $i+1$; $A_{avg}(i)=A_{rms}(i)$

Computing of harmonic:

By FFT (16 bits) 1024 samples on 4 cycles without windowing (CEI 1000 – 4-7). From real and imaginary parts, each bin computed on each phase V_{harm}, U_{harm} and A_{harm} in proportion to the fundamental value and the angles V_{ph}, U_{ph}, and A_{ph} between each bin and the fundamental.

This computing is done by the following principle:

Module in %: $mod_k=\frac{c_k}{c_1}\times 100$

angle in degree: $\varphi_k=arctan\left(\frac{a_k}{b_1}\right)$

c_k is the amplitude of frequency $\mathrm{f_k=\frac{k}{4}f_1}$, F_s is sampled signal, c_o is the DC component, k is the ordinal number (spectral bin).

$$\text{With}\begin{cases} c_k=\left|b_k+ja_k\right|=\sqrt{a_k^2+b_k^2} \\ b_k=\frac{1}{512}\sum_{s=0}^{1024}F_s\times sin\left(\frac{k\pi}{512}s+\varphi_k\right) \\ a_k=\frac{1}{512}\sum_{s=0}^{1024}F_s\times cos\left(\frac{k\pi}{512}s+\varphi_k\right) \\ c_o=\frac{1}{1024}\sum_{s=0}^{1024}F_s \end{cases} \quad (22)$$

Computing of the distortion factor (DF):

There are computed two global values that give the relative quantity of harmonics: total harmonic distortion (THD) against the fundamental and the distortion factor (DF) and DF against the effective value (RMS).[4]

$$V_{thd}(i)=\frac{\sqrt{\frac{1}{2}\sum_{n=2}^{50}V_{harm}(i,n)^2}}{V_{harm}(i)} \quad U_{thd}(i)=\frac{\sqrt{\frac{1}{2}\sum_{n=2}^{50}U_{harm}(i,n)^2}}{U_{harm}(i)}$$

$$A_{thd}(i)=\frac{\sqrt{\frac{1}{2}\sum_{n=2}^{50}A_{harm}(i,n)^2}}{A_{harm}(i)} \quad (23)$$

$$V_{df}(i)=\frac{\sqrt{\frac{1}{2}\sum_{n=2}^{50}Vharm(i,n)^2}}{Vrms(i)};\ U_{df}(i)=\frac{\sqrt{\frac{1}{2}\sum_{n=2}^{50}Uharm(i,n)^2}}{Urms(i)}$$

$$Adf(i)=\frac{\sqrt{\frac{1}{2}\sum_{n=2}^{50}Aharm(i,n)^2}}{Arms(i)} \quad (24)$$

Multiplying the voltage's harmonics factor with the current's harmonics factor, results the power's harmonics factor. Differentiating the voltage's harmonic phase angle with the current's harmonic phase angle, results the power's phase angle.[4][6]

- different ratios

$PF(i)=\frac{W(i)}{VA(i)}$ power factor, phase $i+1$

Cosinus angle between the voltage's fundamental and the phase current $i+1$

$$cos[\varphi(i)]=\frac{\sum_{n=0}^{N-1}VF(i,n)\cdot AF(i,n)}{\sqrt{\sum_{n=0}^{N-1}VF(i,n)^2}\cdot\sqrt{\sum_{n=0}^{N-1}AF(i,n)^2}} \quad (25)$$

Total power factor of various types of energy

$$PF3=\frac{PF(0)+PF(1)+PF(2)}{3} \quad (26)$$

Active energy consumed $i+1$ phase;

$$Wh(0,i)=\sum_{T\,int}\frac{W(i)}{3600} \quad (27)$$

Reactive inductive energy consumed $i+1$ phase;

$$VARhL(0,i)=\sum_{T\,int}\frac{VAR(i)}{3600}\ \text{for}\ VAR(i)\geq 0 \quad (28)$$

Reactive capacitive energy consumed $i+1$ phase.

$$VARhC(0,i)=\sum_{T\,int}\frac{VAR(i)}{3600}\ \text{for}\ VAR(i)\leq 0 \quad (29)$$

The measurements comprised both instantaneous and average values.[4]

First is presented the situation with engine power at low voltage and without charge, without absorbing the current (Fig.5) (Fig.6). It appears that the voltage is almost sinusoidal form.

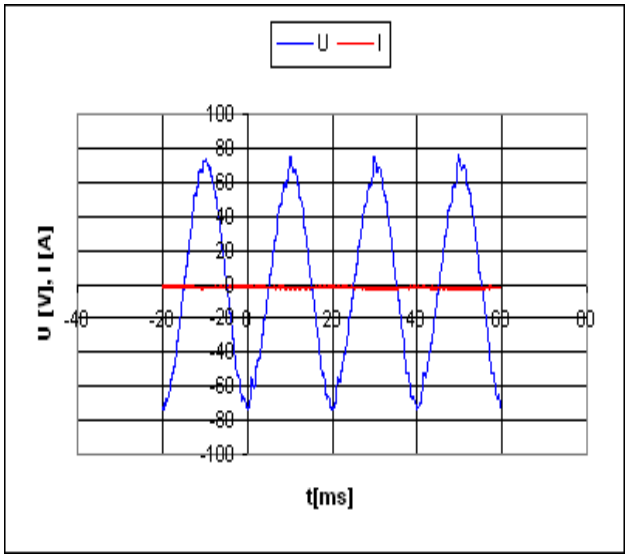

Figure 5. Voltage and current variation shape without supplying excitation

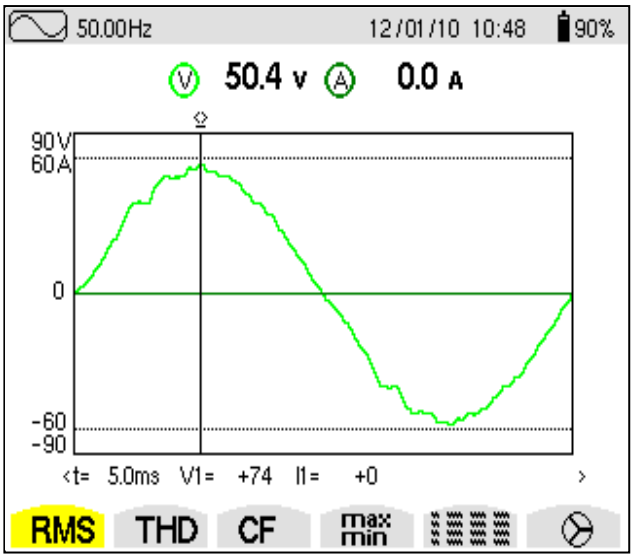

Figure 6. Voltage variation shape for I=0

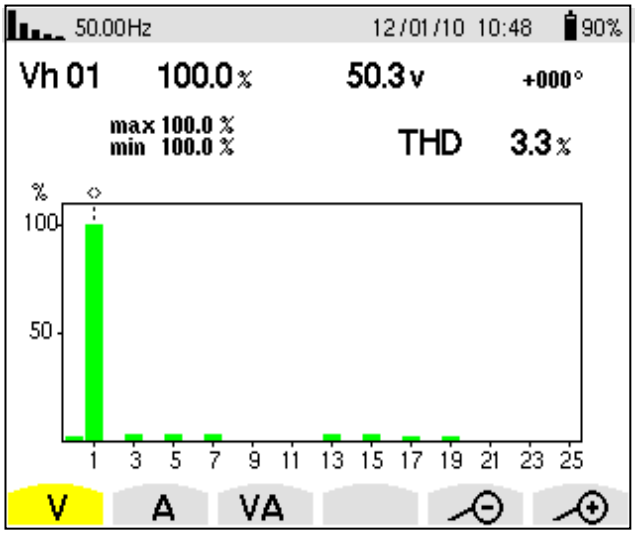

Figure 7. Voltage harmonics values without supplying excitation.

Corresponding to this situation is obtained (fig. 7) a voltage harmonic distortion factor THDU by 3.3% witch is within the range of compatibility. [9][17].

It was registered the current's and voltage's variation from the beginning of the motor's load-up (fig.8), by deforming the voltage and increasing the current (fig.9), where the current reaches a maximum value of 1000A and the voltage has a reduced and very deformed value.[15][18]

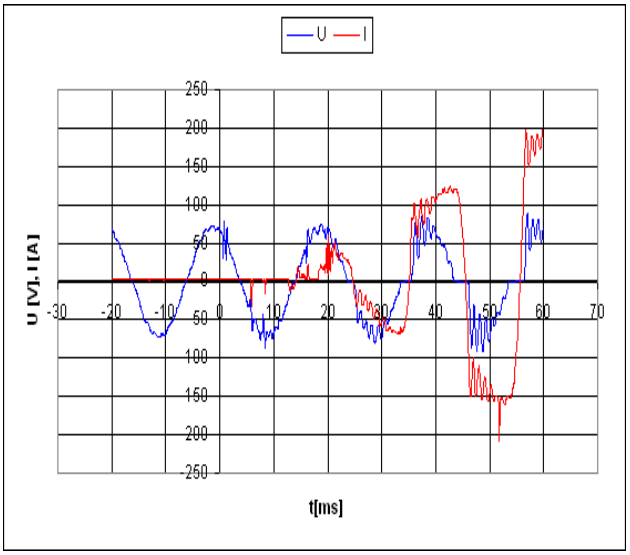

Figure 8. Instantaneous values of voltage and current when entering the short-circuit regime

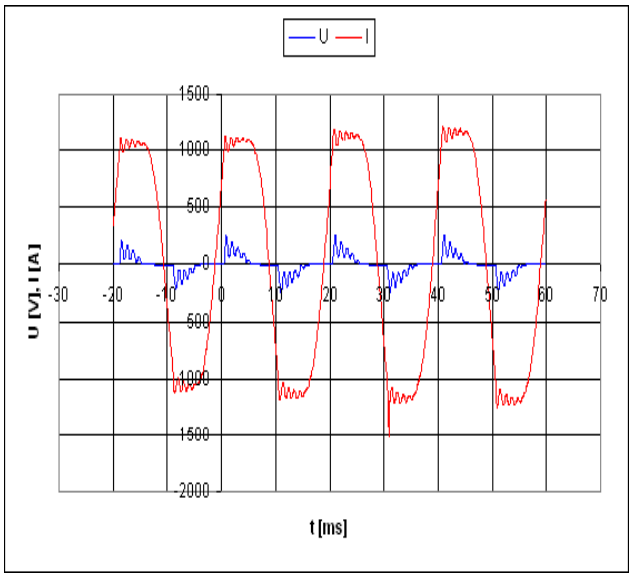

Figure 9. Instantaneous values of voltage and current during the short-circuit regime

At different maximum voltage values and current absorbed by approximately 200V and 800A. (fig. 10) or 100V and 500A (fig. 11) shows a shape almost sinusoidal for the current and a deformation

very pronounced for the voltage.[14][21]

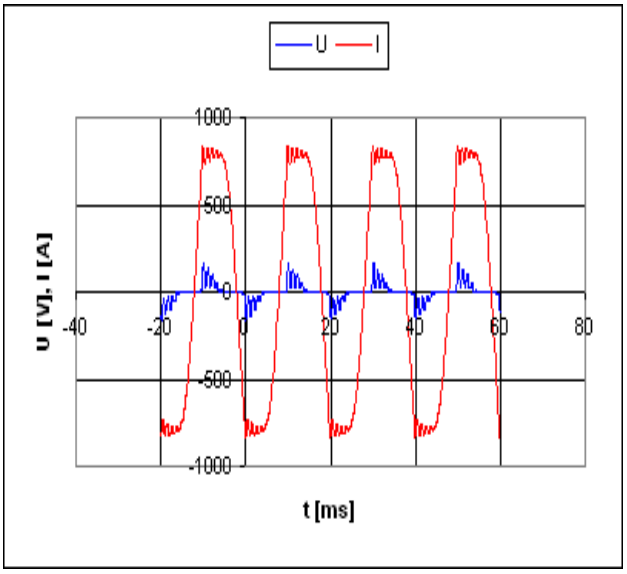

Figure 10.Variation shape for the current and voltage for I_{max}=800A

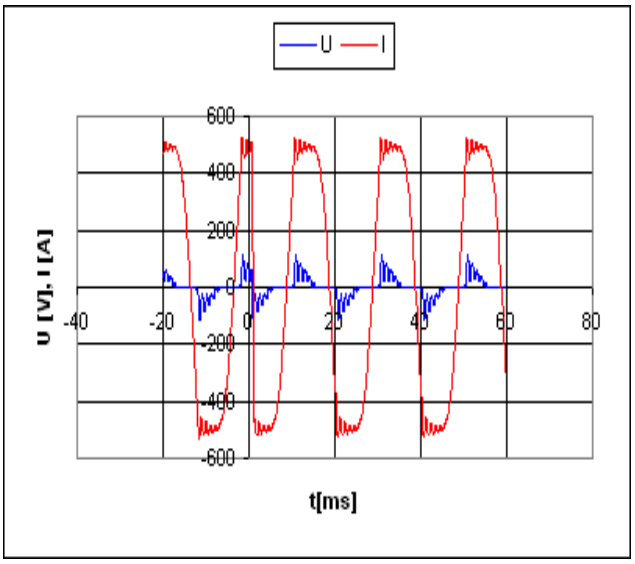

Figure 11. Variation shape for the current and voltage for I_{max}=500A

The representation for the three different values of the absorbed current, respectively for the three voltages different supply values (fig.9, fig.10, fig.11) show similar variation shapes for the three cases as for current as for voltage. [13][16][25]

Voltages variation shapes are strongly deformed because of the system lock rotor, system that we won't meet in real life just accidentally and it has some similar characteristic with starting system with maxim traction load.[10][24]

Current variation shape close to sinusoidal shape is explained by the fact that the engine with the locked rotor acts as a simple inductance.[19]

In this situation, for voltage is obtained a very high THD, around 80% (Fig.12), with important harmonics, even of superior order and a relatively reduced factor for current, of approximately 16% (fig.13).

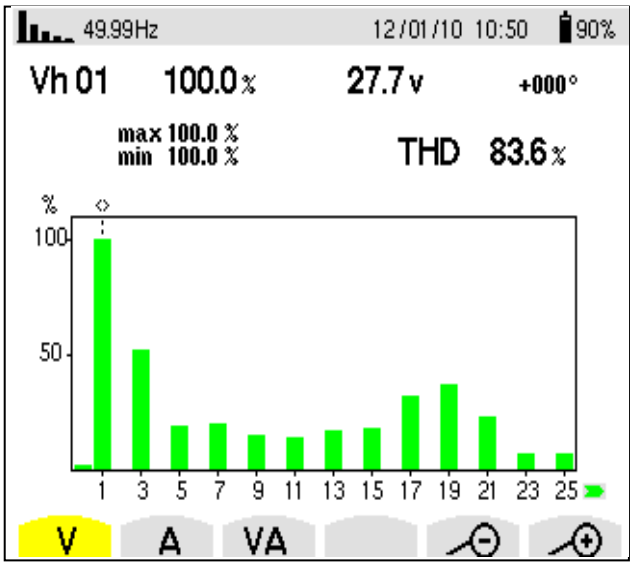

Figure 12. Voltage harmonics' values in short-circuit regime

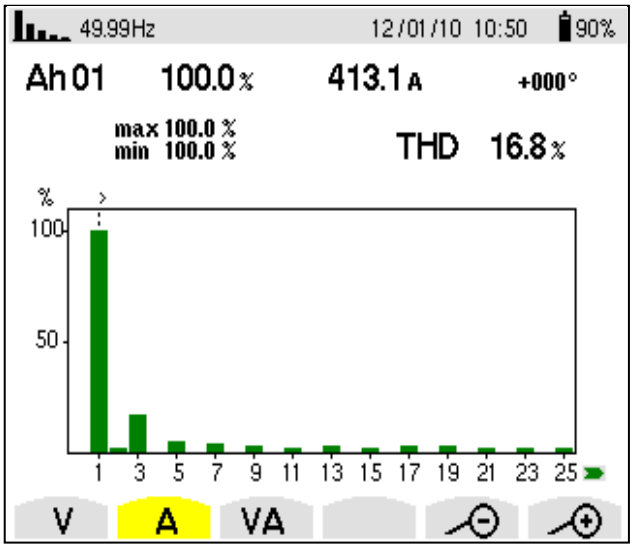

Figure 13. Current harmonics' values in short-circuit regime

From these graphics, one can observe the deeply deforming character of the motors in short-circuit regime, regime that leads to their rapid heating, therefore this situation should be avoided.[7][8]

Currents were determined on three different engines (fig.14) and found a variation almost identical with very small differences, differences that occur because of the construction of engines and power circuits.

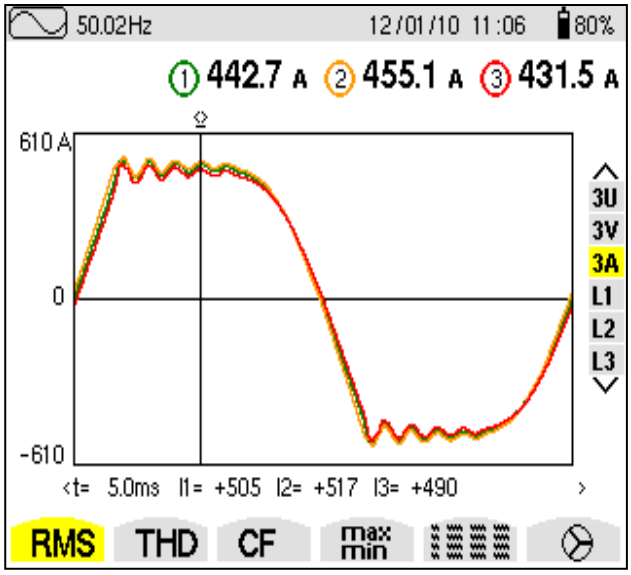

Figure 14. Current variation shape through three traction engines

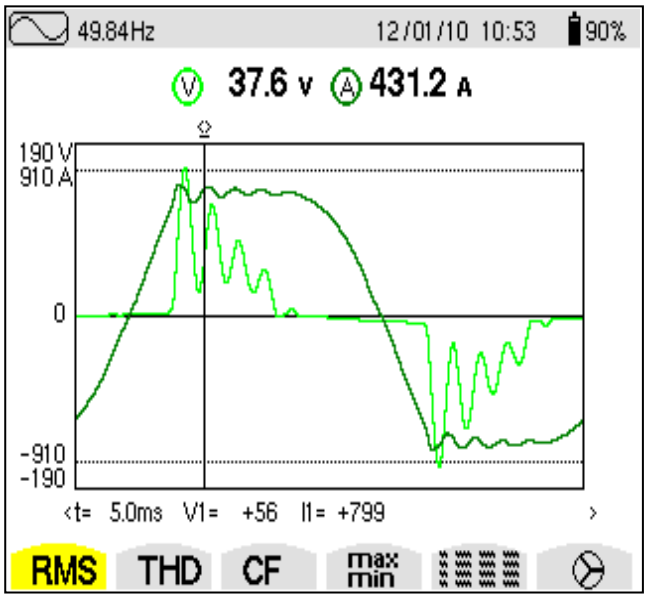

Figure 15. Voltage and current variation shape for I=431,2A

Next is presented current and voltage variation shapes for an engine at different values of current and supply voltage (fig.15, fig.16, fig.17, fig.18).

From their analysis we can observe a very similar variation shape as for the current as for the voltage at very different values of voltage but especially for the absorbed current by the motor stator circuit. [12]

For this case is obtained a voltage-current phase difference of 27^0 (Fig.19), which leads to the power factor's decrease. [5]

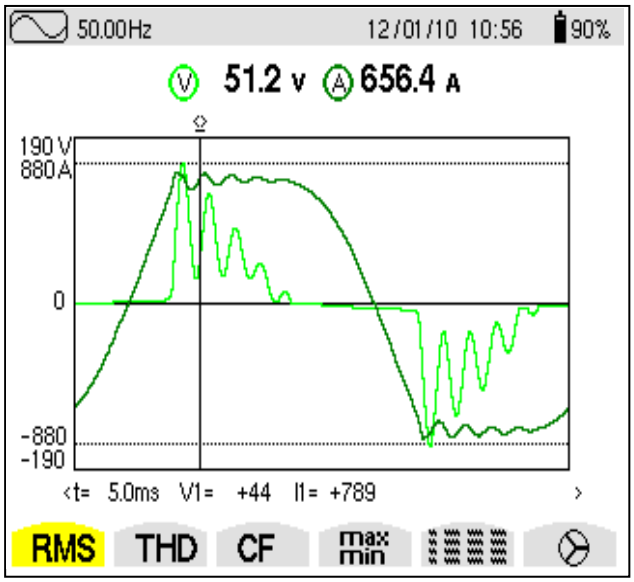

Figure 16. Voltage and current variation shape for I=656,4A

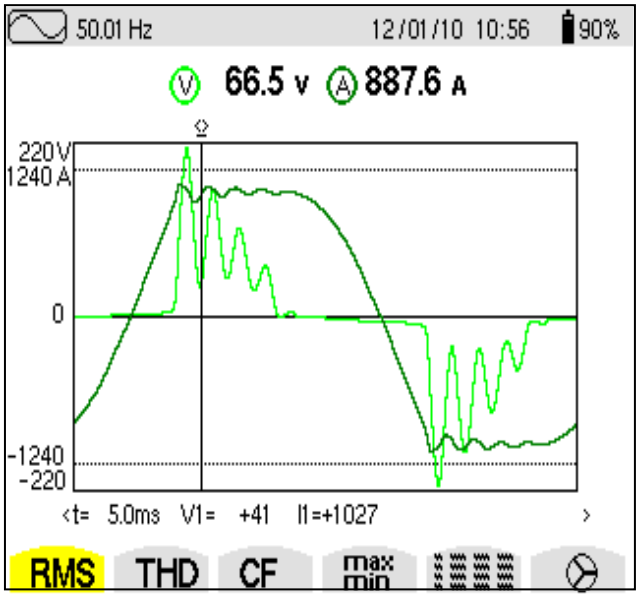

Figure 17. Voltage and current variation shape for I=887,6A

For phase angle result a small change in a current of 1110 (fig. 19) versus current phase angle obtained at 413.8 A (fig. 20), by only 1^0.

This small phase angle difference is explained by the fact that the wheels lock engine does not change the parameters of the circuit when change engine power.

Measurements presented allows to determinate limit values to operate under short circuit current traction motors continuously.

Throw this can be established limit for the measuring apparatus and protective equipment to avoid damaging components of the electric traction vehicles and for them supply installations. [23]

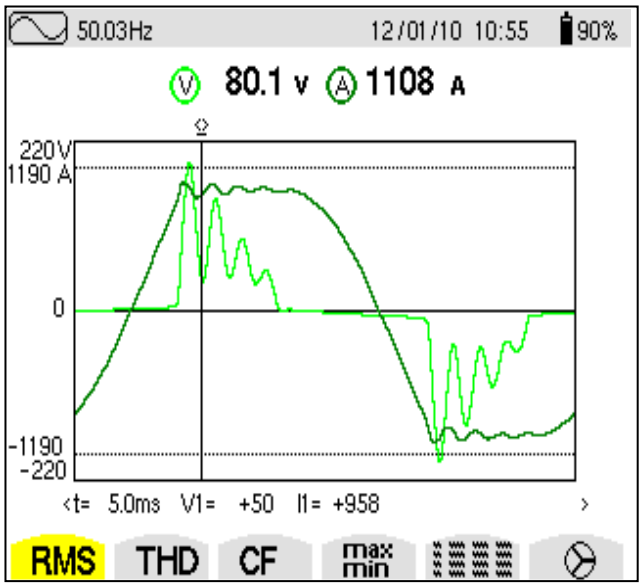

Figure 18. Voltage and current variation shape for I=1108A

Measurements were made for a single engine, observing that the others are behaving at the same as we obtained when we determine current for three different engines. (fig. 14), when we obtained three currents almost identical, the difference being given by their structural characteristics.

Note that as for harmonic voltage as for current the most important is the harmonic order 3, following a decrease in their values and then increasing harmonics order 17 and 19.

Harmonic compensations issues are not counting because this operating system in not normally encountered in service, it should be known for sizing the power supply circuits.

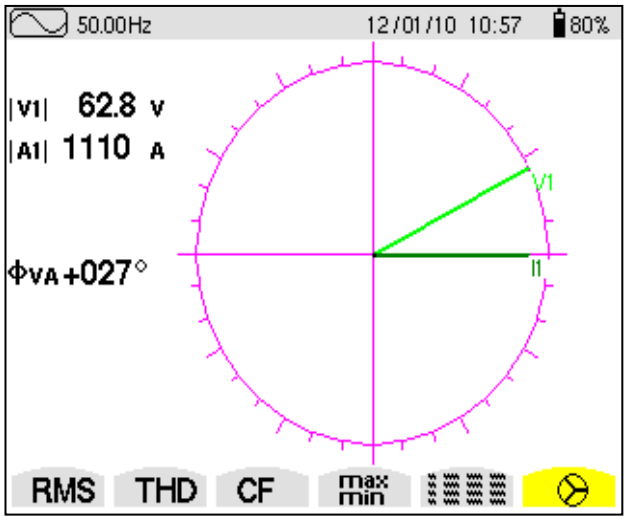

Figure 19. Phase difference U-I in short-circuit regime for I=1110A

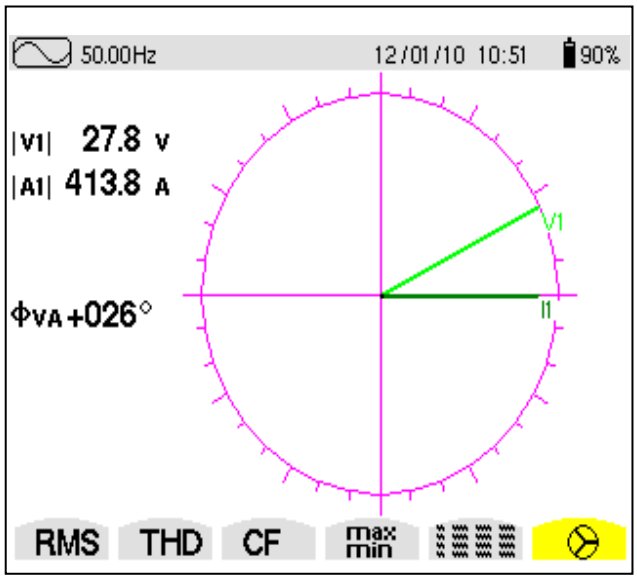

Figure 20 Phase difference U-I in short-circuit regime for I=413,8A

3 Conclusion

Further the measurements performed in case when the d.c. motor's rotor is blocked, so in short-circuit regime, is found a very pronounced deformation of the supply voltage THD>80% and in a small measure, a deformation of the current with a distortion factor THD < 17%.

The same can be found when we analyze the values of the voltage and current harmonics. In voltage's case, the harmonics' values are significant even to the ones of superior order (>40) which are not represented on figure due to the need of its display with a proper clarity.

Almost sinusoidal current shape and a very deformed voltage shape reveal similar behavior in the engine operating mode, with the mention that differ only currents and voltage values as their harmonics values, and variation shape is identical for al the cases analyzed.

There is a random variation amortized as for the voltage as for the current, variation determined by the bridge rectifier and the connection mode excitation circuits of each engine, engine witch is made serial at the start with another of the six with witch the vehicle traction is equipped .

Another important factor represents the phase difference increase between U and I, which leads automatically to the reactive power's increase and, thus, to the aggravation of the supply grid's regime.

The reactive power due to the phase difference is added to the reactive power due to the harmonics, resulting an unfavorable situation that should be avoided as much as possible.

References:

[1]Adrian Buta, Adrian Pană, *Symmetrization of the Electric Distribution Grids' Load*, „University Horizons", Timişoara, 2000.

[2] Steimel A., *Electric Traction Motive-Power and Enrgy Supply. Basics and Practical Experience*, Oldenbourg Industrie Gmbh, 2008.

[3]Ioan Boldea I, *Transformers and electric machines*, Academy's Publishing House, Bucharest 1991;

[4]C.A. 8334B, *Three Phase Power Quality Analyser*, Chauvin Arnaux, France, 2007.

[5]Pănoiu, M., Pănoiu, C., Osaci, M., Muscalagiu, I., *Simulation result about harmonics filtering using measurement of some electrical items in electrical installation on UHP EAF*, WSEAS Transactions on Circuits and Systems 7 (1), pp. 22-31, ian 2008;

[6]Angela Iagar, Gabriel Nicolae Popa, Ioan Şora, *Analysis of electromagnetic pollution produced by line frequency coreless induction furnaces*, Wseas Transactions on Systems, January2009,volume 8, Issue 1, ISSN 1109-2777;

[7]Corneliu Botan, Vasile Horga, Florin Ostafi, Marcel Ratoi, *Minimum Energy and Minimum Time Control of Electrical Drive Systems*, WSEAS Transactions on Power Systems, Issue 4, Volume 3, April 2008, ISSN: 1790-5060.

[8]Alan k. Wallace, Rene Spee, *The Effects of Motor Parameters on the Performance of Brushless d.c. Drives*, IEEE Transactions on Power Electronics, vol.5, no.1, January 1990;

[9]Popescu M., Bitoleanu A., Dobriceanu M., "*Harmonic Current Reduction in Railway Systems*", WSEAS Transactions on Systems, Issue 7, Vol. 7, iulie 2008, ISSN: 1109-2777, pp. 689-698.

[10]Jarou T., Cherkaoui M., Maaroufi M., *Contribution to the controlling of the shunt active power filter to compensate for the harmonics, unbalanced currents and reactive power*, Proc. WSEAS/ IASME Int. Conf. on Electric Power Systems, High Voltages, Electric Machines, Tenerife, Spain, 2006, pp. 263 - 269.

[11] Han Y., Mansoor, Yao G., Zhou L.D., Chen C., *Harmonic Mitigation of Residential Distribution System using a Novel Hybrid Active Power Filter*, WSEAS Transactions on Power Systems, Vol.2, Issue 12, 2007, pp. 255 - 260.

[12]Chymera M., Renfrew A.C., Barnes M., *Railway modelling for power quality analysis*, WIT Transactions on The Built Environment, Vol.88, 2006.

[13] Lee H., Kim G., Oh S., Jang G., Kwon S., *Fault analysis of Korean AC electric railway system*, Electric Power Systems Research, Vol. 76, Issue 5, 2006, pp 317-326.

[14]Liu W., Cheng G.W., Deng C.N., "*Analysis of electric vehicle's driving motor*", Motor Technology, pp. 26–28, 2006.

[15]Milea L., *Deforming system analysis in the power system – thesis,* Universitatea Politehnica Timisoara, Fac. De Electrotehnică, 1998.

[16] Nicolae P.M., Power quality in limited power systems, Editure Tehnica, Bucuresti ,1998.

[17]Popescu M., Bitoleanu Al., Dobriceanu M., „*Case Study Survey of Harmonic Pollution Generated by Railway Systems and Filtering Solutions*", 12 th WSEAS International Conference on Systems, Heraklion, Greece, July, 22-24, 2008, pp. 210 ÷ 215, ISBN 978-960-6766-83-1, ISSN 1970-2769.

[18] Shaofeng X., Qunzhan L., *A Practical Method for Assessment of Harmonic Emission of Electrified Railway*, 32nd Annual Conference on IEEE Industrial Electronics, Paris, Nov. 2006, ISSN: 1553-572X, pp. 2827-2831.

[19]Tan P.C., Loh P.C., Holmes D.G., *Optimal Impedance Termination of 25-kV Electrified Railway Systems for Improved Power Quality*, IEEE Trans. on Power Delivery, Vol.20, No.2, 2005, pp. 1703-1710.

[20]Ţugulea A., Considerations on the energy effects of deformed, Energetic, vol. 34, Nr. 1, pg. 27-31, 1986.

[21]Ţugulea A., Considerations on the energy effects of the unsymmetrical three phase systems harmonic schemes, Energetic, vol.34, nr.3, 1986, pp.121-129.

[22]Liu W., Cheng G.W., Deng C.N., "*Analysis of electric vehicle's driving motor*", Motor Technology, pp. 26–28, 2006.

[23] Oettmeier M., Heising C., Staudt V., Steimel A., *Dead-Beat Control Algorithm for Single-Phase 50-kW AC Railway Grid Representation*, IEEE Transactions on Power Electronics, Vol. 25, Issue 5, pp. 1184-1192, 2010.

[24] Subjak J., Mcquilkin J., *Harmonics – Causes, Effects, Measurements, and Analysis: An Update,* IEEE Transactions on Industry Applications, Nr. 6.

[25] ***, *Practical definitions for powers in systems with nonsinusoidal waveforms and unbalanced loads,* IEEE Working Group on nonsinusoidal situations: Effects on meter performance and definitions of power, IEEE Transactions on Power Delivery, vol. 11, no. 1, 1998, pg. 79-87.